Modeling of a Solid Oxide Fuel Cell as Part of a Predictive Functional Model for Aerospace Fuel-Cell Systems

Mary Lou Nadeau[1]
Aerodyne Industries, Houston, TX, 77058, USA

Kevin Lange[2]
Jacobs Technology, Houston, Texas, 77058, USA

Thomas Cognata[3]
NASA Johnson Space Center, Houston, Texas, 77058, USA

This paper will discuss initial efforts at developing a parametric fuel cell component model for architecture studies of aerospace systems. Fuel cells historically have been used in spacecraft from the Gemini to the Shuttle era for providing spacecraft power with the added benefit of producing water for crew use. However, there are many potential applications for fuel cells and electrolyzers in spaceflight, including oxygen generation, in-situ resource utilization (ISRU) and propellant production. This proof-of-concept model has been developed using a commercial multiphysics modeling software package. Two-dimensional and one-dimensional isothermal models were created based on a certain SOFC design and results were compared to test data from the real system. Local Butler-Volmer kinetic relations were adjusted, and an effective porous medium approach was taken in order to capture how the many interconnects between cells in the gas channels affected fluid flow. The model was able to reproduce polarization curves derived from test data within around 0.02 Volts for a given current density. This model could be adapted to model a solid oxide electrolyzer, proton exchange membrane fuel cell, or other type of fuel cell technology in order to understand how these types of technologies could fit into broader spacecraft designs and advance the capabilities of spaceflight systems.

Nomenclature

A_{loc}	=	local pre-exponential factor
A_{PNNL}	=	overall pre-exponential factor
BV	=	Butler-Volmer
E_a	=	activation energy
$ECLS$	=	Environmental Control and Life Support
E_{eq}	=	equilibrium potential
$E_{eq,ref}$	=	reference equilibrium potential
F	=	Faraday's constant
H_{gde}	=	electrode thickness
i_{loc}	=	local current density
$ISRU$	=	in-situ resource utilization
K_{eq}	=	water formation equilibrium constant
mA	=	milliamperes
OCV	=	open-cell voltage

[1] Modeling and Simulation Chemical Engineer, 2224 Bay Area Blvd, Houston, TX 77058/JE-5EA.
[2] Engineering Specialist, Engineering Dept., 2224 Bay Area Blvd, Mail Stop JE-5EA.
[3] Fuel Cell Engineer, NASA JSC, 2101 NASA Pkwy, Mail Stop EP311.

PEM	=	Proton exchange membrane
p_i	=	partial pressures of constituent i
$p_{i,ref}$	=	partial pressures of constituent i in the reference state
$PNNL$	=	Pacific Northwest National Laboratory
R	=	universal gas constant
RHE	=	reference hydrogen electrode
$sLpm$	=	standard liters per minute
$SOFC$	=	solid oxide fuel cell
S_V	=	surface area to volume ratio
T	=	temperature in Kelvin
YSZ	=	yttria-stabilized zirconia
ΔG	=	Gibbs free energy of the electrode reaction
γ	=	adjustable exponential factor
η_{loc}	=	activation overpotential
μm	=	micrometer

I. Introduction

FUEL cells have a long history of powering NASA missions and are contenders for integration into the power architecture for the moon and Mars. Proton exchange membrane (PEM) fuel cells were used to power the Gemini V spacecraft in the 1960s.[1] The associated product water also served as a source of potable water for crew. Then, the Apollo missions, Skylab, and Space Shuttle Orbiter leveraged the power of alkaline fuel cells for electricity and water generation.[1] When fuel cells are run in the reverse, i.e., producing hydrogen and oxygen from water and electricity, they are called electrolyzers. Electrolyzers are being considered for in-situ resource utilization (ISRU), which is becoming an important focus area for lunar and mars missions. If used for future missions, electrolyzers could allow for fuel generation after leaving Earth, thus reducing the amount of fuel that would need to be launched for the mission.

Fuel cells also have been of increasing interest for terrestrial applications such as powering cars, trucks, and other vehicles because of their low environmental impact. For that reason, the amount of research into optimization of fuel cells has increased in recent years, with the area of mathematical modeling a focus area of interest. Mathematical models are useful because they can be used to quickly compare expected performance of the fuel cell for integration of the technology into larger systems. The goal of this effort is to create an adaptable fuel cell model that can be integrated into larger power or Environmental Control and Life Support (ECLS) system models. The first phase of this effort, discussed in this paper, was to produce a proof-of-concept analytical predictive model of a solid oxide fuel cell (SOFC). The work has been extended to a second phase in which the component model will be implemented into a system model for parametric analysis. Additionally, the team would also like to develop a model for a PEM fuel cell and incorporate it into the developed model integration schema from the SOFC effort. This paper will discuss the first phase of the effort: development of a proof-of-concept SOFC component model.

II. Background

Fuel cells are electrochemical cells that produce electricity from a fuel and an oxidant, usually hydrogen and air or oxygen. The voltage (and subsequent cell power) associated with the current generation are based on the fuel cell chemistry, design, and operation.[2] There are different types of fuel cells, including PEM, alkaline, and SOFC. SOFCs operate at higher temperatures than PEM or alkaline fuel cells and use extremely thin ceramic electrolytes to conduct oxide ions from the cathode to the anode.[2] Additionally, SOFCs can be manufactured as tubular or planar, rectangular cells, with the fuel and oxidant streams in either co-flow or counter-flow orientations. They have a very long aspect ratio, i.e. the flow direction is much longer than the channel height. This model was developed for a planar, co-flow SOFC, depicted in Figure 1. The dimensions in Figure 1 are not to scale; they have been shortened in the width direction in order to highlight each layer. Additionally, the SOFC modeled in this effort is anode-supported, so the anode in reality is much greater in thickness than the cathode.

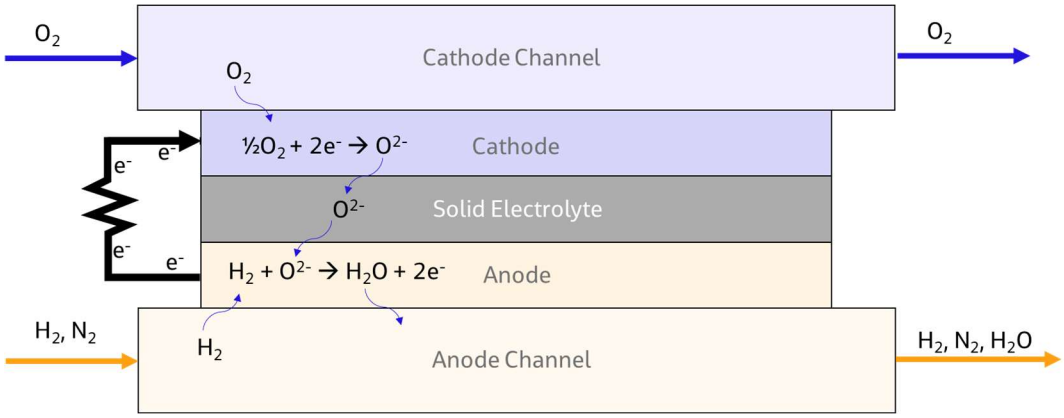

Figure 1. 2D Representation of a planar SOFC and associated chemical reactions.

At the cathode, oxygen from the cathode flow channel gets reduced to oxide ions. Air is often used for the oxidant in terrestrial SOFCs, but for space applications pure oxygen is more common. The oxide ions are conducted through the very thin ceramic electrolyte, where they react with hydrogen at the anode to produce water and electric current. Electrons are conducted through metal interconnects which are not shown in Figure 1 for simplicity.

III. Methodology

Model results were compared to test data from a 30-cell, anode-supported, planar SOFC stack. The cell stack was tested at varying current loads, and the corresponding cell voltages, temperatures, and outlet flow rates were measured. From this data, polarization curves were extracted at two different conditions, Case A and Case B shown in Table 1 below, to compare the data to model results. In Case A, the flow of the H_2/N_2 and O_2 streams were 20.1 sLpm (divided into 30 cells for a cell flow rate of 0.67 sLpm), and the average cell stack temperature was 731 °C. In Case B, the flow of the H_2/N_2 and O_2 streams were 25.1 sLpm (0.84 sLpm to each cell), and the average cell stack temperature was 756 °C.

Table 1. Test Data Cases for Model Comparison.

Case	H_2/N_2 Flow Rate (sLpm)	Average Temperature (°C)
A	20.1	731
B	25.1	756

The component models were developed in a commercial multiphysics modeling software (COMSOL Multiphysics® 6.1) that offers built-in modules and parameter interfaces that can be coupled together to describe complex physical phenomena. Included in these modules is one that describes the electrochemical and flow phenomena in fuel cells and electrolyzers, with specific options for SOFC's and PEM fuel cells. It also has built-in connections to external coding platforms, which could enable integration into larger system models.

Two approaches were used when developing the multiphysics models: one used the built-in hydrogen fuel cell module, and one was constructed from more basic physics components (first principles) to try to better understand the assumptions and limitations of the built-in packages. Additionally, both two-dimensional (2D) (Figure 2) and one-dimensional (1D) (Figure 3) models were developed for both approaches. The 2D models capture the fluid flow phenomena of the oxygen and hydrogen streams along the gas channel and couple that with the mass sources and sinks due to the electrode reactions. The 1D model does not specifically include segments for the gas channels, but instead specifies gas composition and pressure as boundary conditions at the channel/electrode interfaces.

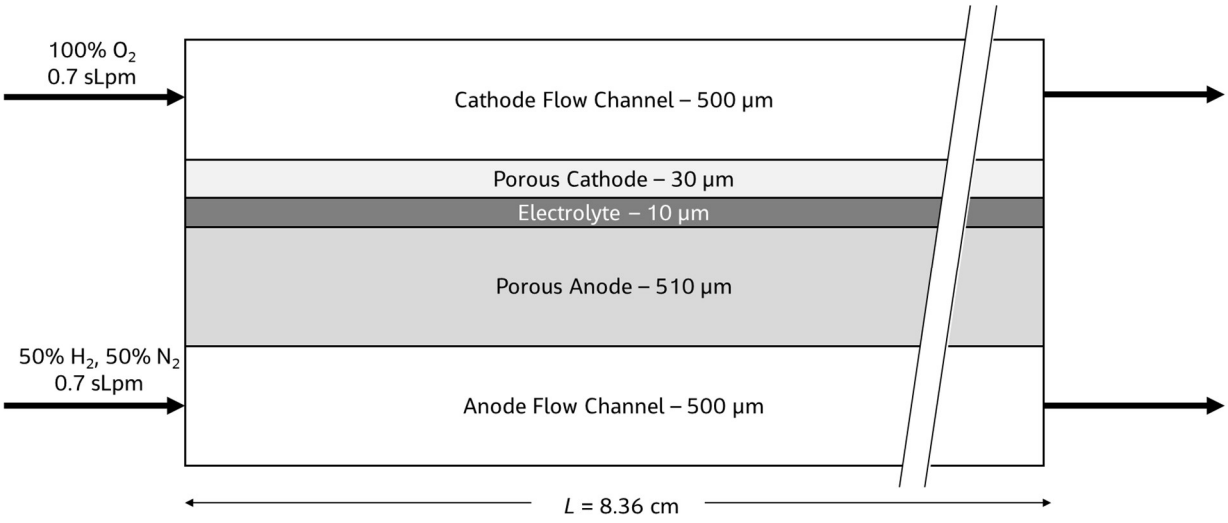

Figure 2. 2D Representation of the SOFC.

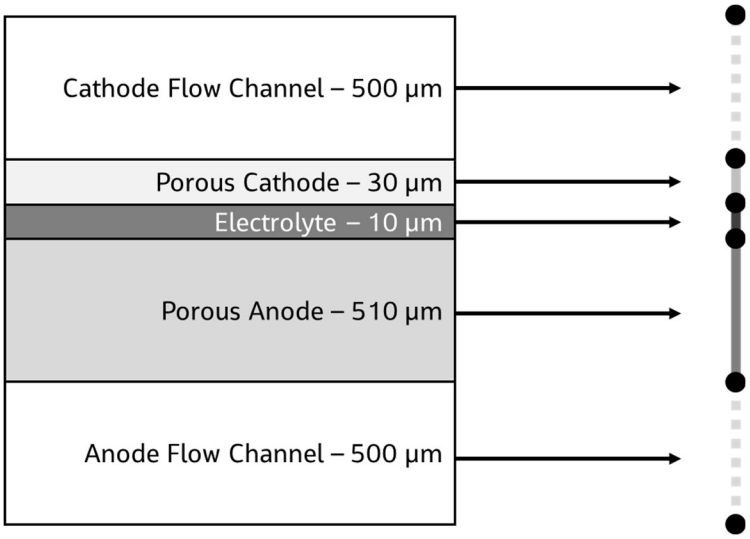

Figure 3. 1D Representation of the SOFC.

Geometric parameters for the Delphi Generation 3 (Gen 3) SOFC were taken from literature.[3] No information was found on the gas channel height, so a value of 0.5 mm was assumed for both the anode and cathode channels. Electrode porosities and electrical conductivity relations were taken from a 1D sub-model developed by Pacific Northwest National Laboratory (PNNL),[4] and the ionic conductivity of the yttria-stabilized zirconia (YSZ) electrolyte is built into the multiphysics software. To account for the flow obstruction due to the interconnects in the anode and cathode flow channels, these channels were modeled as porous media, with an effective porosity estimated from the geometry to be 0.7.

Local Butler-Volmer (BV) reaction kinetic relations were derived from integrated anode and cathode relations in the PNNL sub-model by matching behavior of the 1D model and PNNL models at low current density using the effective kinetic thickness of the anode and cathode electrodes as adjustable parameters. These relations were then applied to the 2D model without further modification.

IV. Results

Results from the models created from the first approach (built-in hydrogen fuel cell module) will be discussed in Section A, and results from the second approach (building up from first principles) will be discussed in Section B.

A. Hydrogen Fuel Cell Module Results

Example plots generated from the 2D model built from the fuel cell module are shown in Figure 4 and Figure 5 below. In the figures, the gas streams enter the channels from the left and exit on the right, with the same orientation of cell layers as depicted in Figure 2 from the previous section. The results from the 2D model in Figure 4 show reasonable velocity fields and pressure drops down each gas channel.

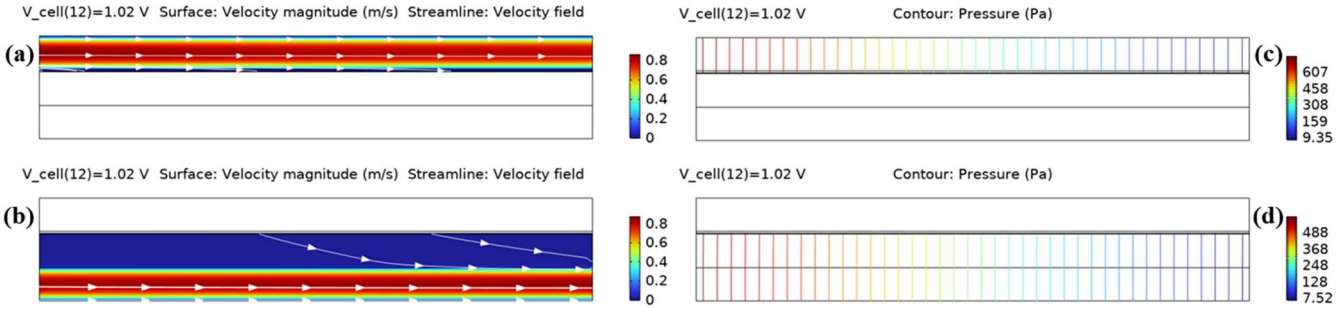

Figure 4. Velocity fields and pressure drops in the anode, cathode, and their flow channels at a cell voltage of 1.02 V. *Velocity fields are depicted in (a) the cathode and cathode gas channel, with the magnitude depicted by color in m/s on a scale of 0 (blue) to 0.8 (red), and (b) the anode and anode gas channel on the same scale. The pressure drops are depicted in (c) the cathode and cathode gas channel in Pa from a scale of 9.35 (blue) to 607 (red) and (d) the anode and anode gas channel in Pa from a scale of 7.52 (blue) to 488 (red).*

Figure 5 shows the mole fraction of hydrogen (which reflects the conversion of hydrogen to water) on the anode side at increasing current densities. The higher the current density, the more hydrogen reacts, as expected.

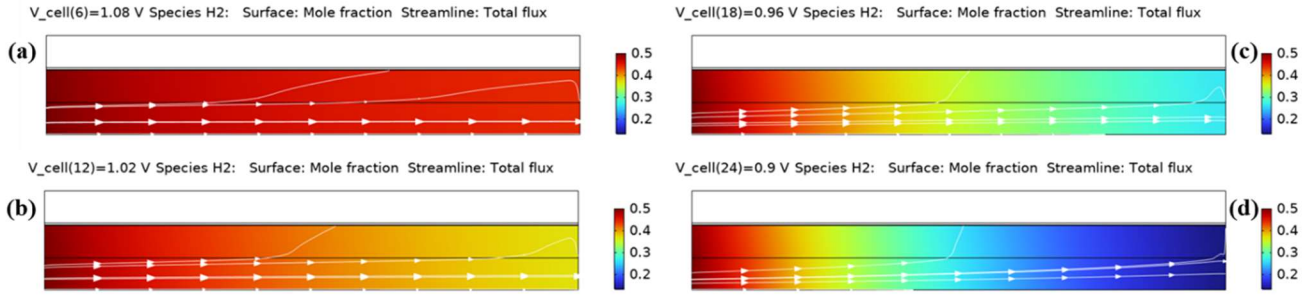

Figure 5. Hydrogen mole fraction in the anode and anode gas channel at increasing cell current density. *The current densities of each plot are as follows: (a) 56 mA/cm^2, (b) 125 mA/cm^2, (c) 224 mA/cm^2, and (d) 349 mA/cm^2.*

Polarization curves for the two test conditions were plotted and compared with test data in Figure 6. The test conditions flow rates and temperatures are listed in Table 1 in Section III. For each case, the shape of the model curves closely follows the shape of the test results, however, the model curves are offset by about 0.02 V in both. This offset could be partially explained by possible differences in temperature from the actual cells and the reported thermocouple value, the lack of incorporation of heat transfer into the model, or other data-related uncertainties. Other potential sources of offset from the theoretical open-cell voltage (OCV) include internal currents and gas leakage across the electrolyte.[5,6]

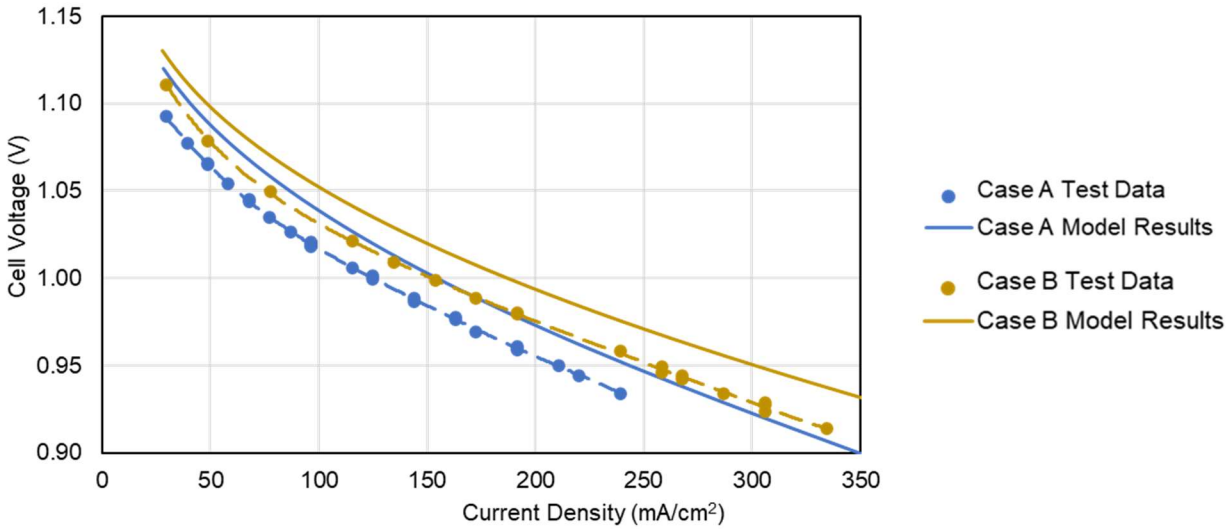

Figure 6. Polarization Curve from the 2D model built from the fuel cell module compared to test data.

Finally, power curves for the two test cases are shown in Figure 7 below.

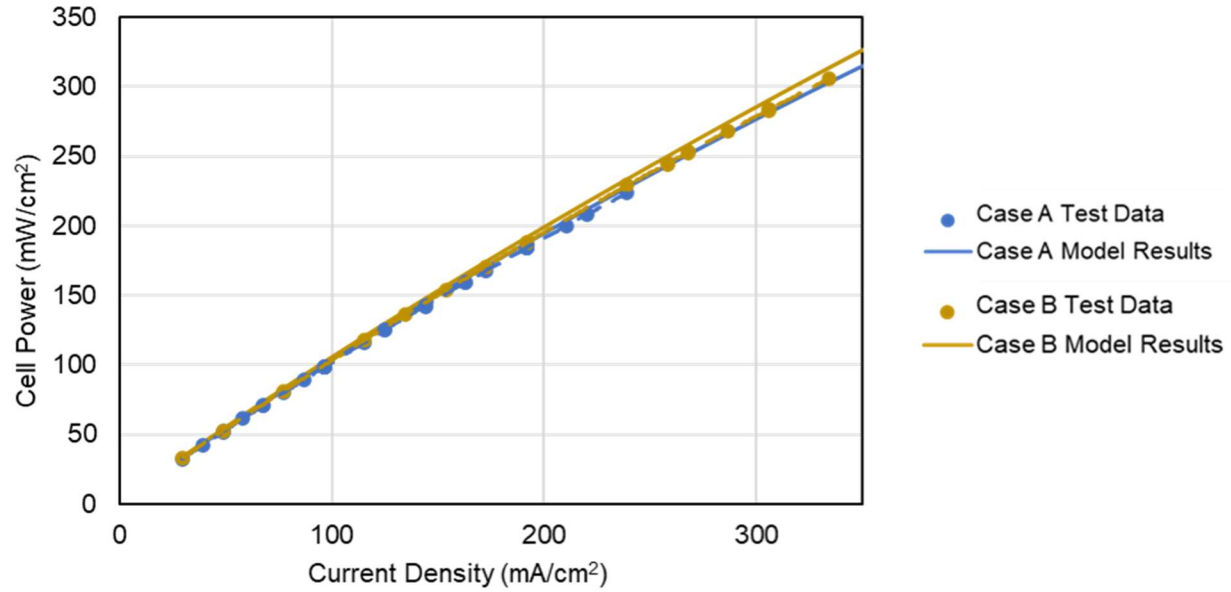

Figure 7. Power curves from the 2D model built from the fuel cell module compared to test data.

The 1D model would need to be coupled with a separate coding platform to iteratively solve the flow field along the axial direction of the gas flow given the electrochemical solution at each axial node. It was developed, in part, to compare results to the 1D PNNL sub-model mentioned earlier.[4] The PNNL sub-model, provided as an example VoltageOnCurrent routine for the 2D SOFC-MP model, was based on an existing PNNL spreadsheet model. By adjusting the effective kinetic thickness of the anode and cathode electrodes, the behavior between the multiphysics model and the PNNL model were matched so that an equivalent expression for the Butler-Volmer (BV) kinetics could be input into the multiphysics model. This involved relating the overall (integral) anode and cathode BV kinetic expressions of the PNNL model to the local BV kinetic expressions of the multiphysics model. The relation between local current density (i_{loc}) and activation overpotential (η_{loc}) in the multiphysics model are described in the following equations:

- Anode:

$$\boldsymbol{i_{\mathrm{loc},a} = A_{\mathrm{loc},a} \exp\left(-\frac{E_a}{RT}\right)\left(\frac{p_{\mathrm{H_2O}}}{K_{\mathrm{eq}} p_{\mathrm{H_2}}}\right)^{2\gamma_a}\left[\exp\left(\frac{F\eta_{\mathrm{loc},a}}{RT}\right) - \exp\left(-\frac{F\eta_{\mathrm{loc},a}}{RT}\right)\right]} \quad (1)$$

- Cathode:

$$i_{\mathrm{loc},c} = A_{\mathrm{loc},c} \exp\left(-\frac{E_c}{RT}\right)\left(p_{\mathrm{O_2}}\right)^{\gamma_c}\left[\exp\left(\frac{2F\eta_{\mathrm{loc},c}}{RT}\right) - \exp\left(-\frac{2F\eta_{\mathrm{loc},c}}{RT}\right)\right] \quad (2)$$

Here, the subscripts "a" and "c" refer to anode and cathode, respectively. E_a is the activation energy, R is the universal gas constant, T is the temperature in Kelvin, F is Farday's constant, $p_{\mathrm{H_2}}$ and $p_{\mathrm{H_2O}}$ are the partial pressures of hydrogen and water, respectively, K_{eq} is the water formation equilibrium constant, and γ is an adjustable exponential factor. At low current density, the BV relations linearize and the local pre-exponential factors $A_{a,\mathrm{loc}}$ and $A_{c,\mathrm{loc}}$ can be related to the overall pre-exponential factors $A_{a,\mathrm{PNNL}}$ and $A_{c,\mathrm{PNNL}}$, the electrode surface area to volume ratio (S_{V}), and the electrode thickness (H_{gde}), as shown in the equations below.

$$A_{a,\mathrm{loc}} = \frac{A_{a,\mathrm{PNNL}}\left(\frac{p_{\mathrm{H_2O,in}}}{p_{\mathrm{H_2,in}}}\right)^{2\gamma_a}\eta_{a,\mathrm{PNNL}}}{S_{\mathrm{V},a}H_{\mathrm{gde},a}\int\left(\frac{p_{\mathrm{H_2O,}}}{p_{\mathrm{H_2}}}\right)^{2\gamma_a}\eta_{\mathrm{loc},a}dx_{\mathrm{gde},a}} \quad (3)$$

$$A_{c,\mathrm{loc}} = \frac{A_{c,\,\mathrm{PNNL}}\left(p_{\mathrm{O_2,in}}\right)^{\gamma_c}\eta_{c,\mathrm{PNNL}}}{S_{\mathrm{V},c}H_{\mathrm{gde},c}\int\left(p_{\mathrm{O_2}}\right)^{\gamma_c}\eta_{\mathrm{loc},c}dx_{\mathrm{gde},c}} \quad (4)$$

Alternatively, the actual electrode thickness (H_{gde}) can be replaced with an effective electrode thickness to match the overall pre-exponential factor.

Thus, using the equations above, the effective electrode thickness parameters were estimated by matching the behavior of the 1D PNNL model results to the results from the 1D Multiphysics software results, shown in Figure 8. The effective thickness for each was determined to be 13.75 mm.

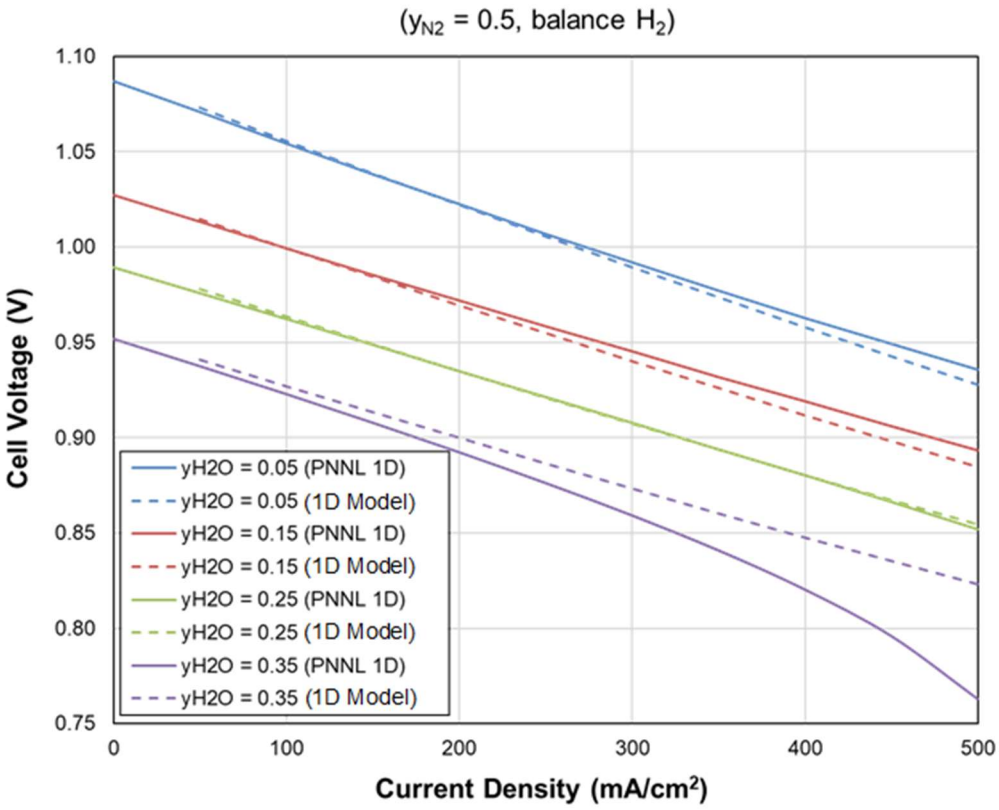

Figure 8. Comparison of 1D Models with PNNL Butler-Volmer Kinetics.

B. First Principles Results

The model built up from first principles did not provide acceptable results at the writing of this paper. When the customized expression for exchange current density was implemented into the model, the solution failed to converge. The model had converged previously with the Multiphysics software's built-in exchange current density expression (based on mass action), however, when the custom expression built from the PNNL model[4] was implemented, the model failed to converge. This expression was used to generate the plots that closely matched test data from the fuel cell module approach (described in Subsection B), so efforts were made to understand why it did not work the same for this approach.

In troubleshooting, the main difference between the two approaches was in the definition of the equilibrium potential in the Nernst Equation when specifying the electrode reaction. The Nernst Equation (Equation 5) specifies the equilibrium potential, E_{eq}, in both the built-in module and the first principles model.

$$\boldsymbol{E_{eq,a} = E_{eq,ref,a} - \frac{RT}{2F} ln \left[\left(\frac{p_{H_2}}{p_{H_2,ref}} \right) \left(\frac{p_{H_2O,ref}}{p_{H_2O}} \right) \right]} \tag{5}$$

Here, the "a" subscript indicates the anode, $E_{eq,ref}$ is the reference equilibrium potential, R is the universal gas constant, T is the temperature in Kelvin, F is Faraday's constant, p_{H_2} and p_{H_2O} are the partial pressures of hydrogen and water, respectively, and $p_{H_2,ref}$ and $p_{H_2O,ref}$ are the partial pressures of hydrogen and water in the reference state, respectively. The difference between the two approaches is that in the fuel cell module approach, the reference equilibrium potential, $E_{eq,ref}$, is defined against a standard reference hydrogen electrode (RHE), as shown in Equation 6, while the first principles approach did not include this, as shown in Equation 7.

$$\boldsymbol{E_{eq,ref,a} = -\frac{\Delta G_a}{2F} - E_{eq,RHE} - \frac{RT}{2F} ln \left(\frac{p_{H_2,ref}}{p_{H_2O,ref}} \right)} \tag{6}$$

$$E_{eq,ref,a} = -\frac{\Delta G_a}{2F} \tag{7}$$

Here, ΔG_a is the Gibbs free energy of the anode electrode reaction. The effect is that the magnitude of $E_{eq,a}$ in the fuel cell module approach is close to zero (-0.12 V), while the magnitude of $E_{eq,a}$ in the first principles model is -1.68 V. When the value of $E_{eq,a}$ in the first principles approach is manually changed to a user-defined value of -0.12 V, as seen in the fuel cell module approach, the model converges and a polarization curve is able to be generated, shown below in Figure 9. However, since the entire expression for $E_{eq,a}$ was changed from the Nernst Equation to a constant value, the equilibrium potential no longer is concentration dependent, and the model still does not match up with the built-in fuel cell module results.

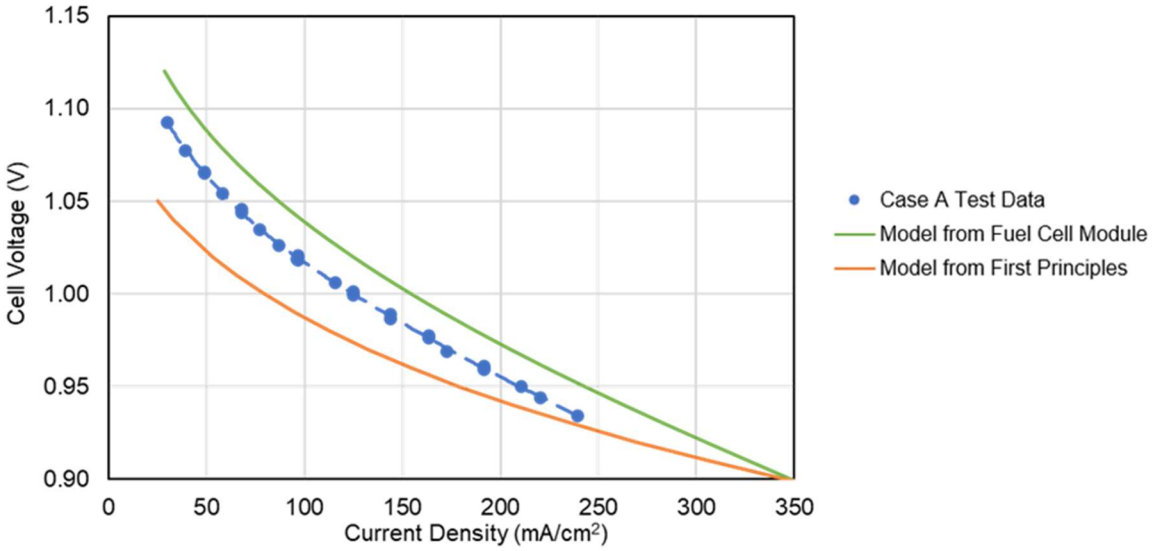

Figure 9. Polarization curve of First Principles Model compared with Fuel Cell Module Results for Case A.

V. Discussion and Phase II Planned Activities

The results of the built-in fuel cell module were satisfactory to close out Phase I of this effort. The 1D model developed would need to be coupled with a separate coding platform to iteratively solve the flow field along the axial direction of the gas flow given the electrochemical solution at each axial node. A comparison in solution speed and accuracy between the 1D approach and the 2D approach is planned for Phase II, with interest in integrability into system models. Further troubleshooting of the first-principles approach is underway during Phase II. Additionally, a rudimentary interface between the component model in the Multiphysics software and other modeling languages was developed, so that polarization curves could be generated based on different inputs of cell temperature, gas flow rates, and current density in the cell. This interface will be improved upon in Phase II, and reformatted to be integrable with existing system models. Once the interface is established, a component model for a PEM fuel cell is planned to be developed as well that could be incorporated similarly into an overall power architecture system model.

VI. Conclusion

This modeling effort produced proof-of-concept models for operation of a SOFC of a given geometry and cell design. These component models can be integrated into system models to run parametric analyses and inform overall system design for future NASA missions. When determining the overall power architecture of lunar and Martian surface operations, having system models that describe the effect of each component is a powerful tool that provides insight into how changes in one component could affect another when testing is not available. Fuel cells and electrolyzers are promising technologies that could benefit human and robotic exploration of the moon and Mars.

Acknowledgments

The authors would like to acknowledge funding from the Power and Propulsion Division at the Johnson Space Center.

References

[1]Burke, K., "Fuel Cells for Space Science Applications," AIAA–2003–5938, NASA/TM—2003-212730, Nov. 2003.

[2]Guzik, M. et al., "Regenerative Fuel Cell Power Systems for Lunar and Martian Surface Exploration," AIAA Space, Orlando, FL, Sep. 2017.

[3]Mukerjee, S., Haltiner, K., Kerr, R., Kim, J., and Sprenkle, V., "Latest Update on Delphi's Solid Oxide Fuel Cell Stack for Transportation and Stationary Applications," ECS Transactions, Vol. 35 (1), 2011, pp. 139-146. DOI:10.1149/1.3569988.

[4]Koeppel, B., Lai, K., and Khaleel, M., "SOFC-MP 2D User Manual," PNNL-20433, Pacific Northwest National Laboratory, May 2011, Appendix C.

[5]Chick, L., Stevenson, J., and Williford, R., "Spreadsheet Model of SOFC Electrochemical Performance," Pacific Northwest National Laboratory, Aug. 29, 2003.

[6]Bove, R., Lunghi, P., and Sammes, N., "SOFC mathematic model for systems simulations. Part one: from a micro-detailed to macro-black-box model," International Journal of Hydrogen Energy, Vol. 30, 2005, pp. 181 – 187. DOI:10.1016/j.ijhydene.2004.04.008.